35th Annual International Conference of the IEEE EMBS
Osaka, Japan, 3 - 7 July, 2013

Reference-Free Harmonic Regression Technique to Remove EEG-fMRI Ballistocardiogram Artifacts

Pavitra Krishnaswamy[1,*], Giorgio Bonmassar[2], Patrick L. Purdon[3], Emery N. Brown[1,3,4,*]

Abstract— **Obtaining high quality electroencephalogram (EEG) data simultaneously with functional MRI (fMRI) recordings is increasingly relevant for the study of cognitive and clinical brain states - as EEG-fMRI offers uniquely high spatiotemporal resolution imaging of brain activity. However, the utility of this technique is limited by ballistocardiogram (BCG) artifacts induced in the EEG by cardiac pulsation and head movement inside the magnetic field. In this paper, we introduce a novel model-based harmonic regression technique to remove BCG artifacts from EEG recorded in the MR scanner. Our technique uses physically motivated parametric models of the BCG artifact and the true EEG signal, and incorporates maximum likelihood approaches to identify model parameters, estimate and subtract the BCG from corrupted EEG measurements. We show that this method effectively removes BCG artifacts from EEG recorded in the MR scanner, restores simulated oscillatory signatures and enables over 20-fold improvement in SNR in bands of interest. Further, unlike common BCG removal techniques that rely on cardiac or motion reference signals, our approach is reference-free and thus is useful when reference signals are corrupted or difficult to acquire.**

I. Introduction

Electroencephalogram (EEG) recorded in the MR scanner offers a means to enhance the utility of functional MRI (fMRI) - as it provides high temporal resolution recordings of brain electrical activity to complement high spatial resolution fMRI-BOLD measurements of regional neuronal substrates. Thus, obtaining high quality EEG recordings in the MR scanner is important for studies of brain oscillations in cognitive and clinical states such as sleep, attention, and anesthesia. However, the utility of this technique is fundamentally limited by ballistocardiogram (BCG) artifacts corrupting EEG recorded in the MR scanner.

The BCG artifact is induced in the EEG primarily by cardiac and blood flow related pulsatile motion of the head and scalp electrodes in the static magnetic field [1]. The BCG has significantly larger amplitudes (150-200 uV at 1.5 T) than underlying EEG activity (10-100 uV), can obscure EEG activity upto 20 Hz [1] and thus lowers specificity and sensitivity of EEG recorded in the MR scanner. Further, variations in heart rate, blood pressure and the resulting pulsatile head motion cause variations in the shape, timing and intensity of the BCG artifact [2], [3] - making the removal of this artifact very challenging.

[1]*Harvard-MIT Health Sciences and Technology, USA*
[2]*Department of Radiology*
[3]*Department of Anesthesia, Critical Care & Pain Medicine Massachusetts General Hospital & Harvard Medical School, USA*
[4]*Brain & Cognitive Sciences, Massachusetts Institute of Technology, USA*
[*]*Correspondence: pavitrak@mit.edu, enbrown1@mit.edu*
NIH Grants: DP2-OD003646, TR01-GM104948 and R01-EB006385 (Brown); DP2-OD006454 and K25-NS057580 (Purdon)

Several BCG removal techniques have been proposed. Commonly, a reference signal like the electrocardiogram (ECG) or a motion sensor is used to estimate a BCG template waveform, and subtract this template from the contaminated EEG [1], [2], [4]. However, these techniques rely on high quality ECG or motion data suitable for robust peak detection and/or adaptive filtering, but often it is hard to acquire clean reference signals especially in magnetic fields $> 1.5\,\mathrm{T}$ or during long recordings. To overcome this, reference-free BCG removal methods such as ICA and wavelet basis decompositions have been explored [5]–[7]. These approaches rely on separability between the true EEG signal and the BCG artifact in amplitude, time and/or frequency - but often many basis elements contain substantial overlap between signal and artifact in these domains [1], [2], [8]. This skews the separation and necessitates significant post-algorithmic-processing and subjective case-specific criteria defining which basis elements should be excluded as "artifact" and which ones should be retained as "true EEG signal" [7]. Thus, we need an approach that can remove the BCG artifact without the need for a reference signal or subjective separation criteria.

In this work, we propose a novel reference-free model-based approach which exploits the physical and physiological features of the BCG artifact. Comparing spectral signatures of BCG-free vs. BCG-corrupted EEG oscillations (Fig. 1A vs. 1B), we observe that the BCG comprises a series of harmonic streaks. This trend is also reflected in time domain which is dominated by pulsatile (comb-like) BCG occurrences that happen to occur with the same period as the heartbeat (Fig. 1C). These observations are consistent with the BCG generation physics [3], [8] and present a natural harmonic basis for specifying the BCG - yet no algorithms explicitly exploit this feature to remove the BCG. We model this temporal structure in the BCG artifact explicitly with a harmonic series, and also model oscillatory dynamics in the true EEG signal with an autoregressive (AR) series. Since the model specifies the template for the BCG, there is no need for a reference signal. Further, our parametric model forms are specific yet loose enough to be generalizable and objective while taking the character of the data - hence we do not require subjective or case-specific criteria to deal with the time-frequency overlap between signal and artifact. The problem of estimating and removing the BCG artifact then becomes one of identifying the harmonic and AR parameters to best explain the contaminated EEG data. We develop a maximum likelihood technique to estimate model parameters, and implement it using a Newton's procedure. Finally, we analyze BCG-corrupted EEG data recorded in a 3T scanner to demonstrate the efficacy of our approach.

978-1-4577-0216-7/13/$26.00 ©2013 IEEE

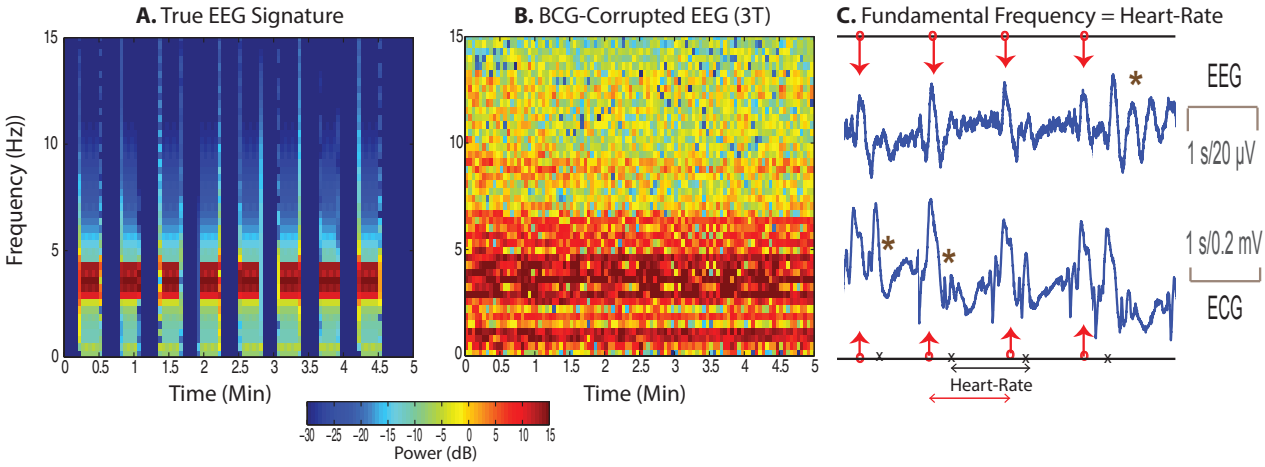

Fig. 1: BCG follows Harmonic Trend with Heart Rate as Fundamental Frequency: (A) High resolution multitaper spectrogram of simulated test oscillatory EEG - delta band power has ON/OFF pattern. (B) High resolution multitaper spectrogram of sum of the simulated test oscillatory EEG in (A) and BCG-corrupted resting state EEG recorded in 3T MR scanner. Artifacts make it difficult to discern ON/OFF delta band pattern in Panel A. (A vs. B) BCG manifests as harmonic streaks in spectrogram. (C) Time series of BCG-corrupted EEG data (from Panel B) vs. simultaneous ECG recording - successive high amplitude BCG combs (indicated by red arrows) have same periodicity as heart-beat. Brown *'s indicate heart cycles where ECG R-wave peaks are hard to identify and/or relation between BCG and ECG peaks varies with time.

II. Methods

A. Data

BCG-corrupted resting state EEG data was collected on two human volunteers in a static 3T magnetic field (Siemens, Erlangen, Germany). The study was approved by the Massachusetts General Hospital Human Research Committee and subjects provided informed written consent. The acquisition hardware comprised an MR compatible, low noise, high dynamic range 24-bit electrophysiological recording system with a 957 Hz sampling rate [9]. Ag/Ag-Cl EEG electrodes were placed in adjacent bipolar pairs in 8 locations across the head. During recording of BCG-corrupted resting state EEG data, study subjects were asked to lay awake and motionless (with eyes open) inside the scanner for 5 minutes. Raw EEG recordings were detrended and put through a low pass filter with 50 Hz cutoff.

To generate a variety of BCG-corrupted EEG oscillation test-cases for developing and benchmarking our algorithm, test oscillatory signals simulating various brain-states of interest in sleep, attention and anesthesia were generated and added to the BCG-corrupted resting state EEG recordings. Each test signal is a sinusoidal oscillation with frequency in the δ band ($1-4$ Hz), θ band ($4-8$ Hz), or α band ($8-12$ Hz). An example test signal with a periodic 17 second ON/17 second OFF pattern is shown in Fig. 1A. This test oscillation is added to the resting state EEG recorded in the MR scanner to produce the corresponding BCG-corrupted EEG oscillation (Fig. 1B). 35 such BCG-corrupted oscillations with varying signal to artifact ratios (SNR) and oscillation frequencies were simulated for each subject - providing a total of 70 test cases for our model-based algorithm.

B. Model

We define a BCG-corrupted EEG oscillation as the sum of the recorded BCG-corrupted resting state EEG and the simulated test oscillatory signal. The BCG-corrupted EEG oscillation can be represented with a harmonic artifact plus colored EEG model. Denoting the BCG-corrupted EEG oscillations from a given channel as the 'measured' data series $y_1, y_2, \ldots, y_{\mathrm{T}}$, we have:

$$y_t = s_t + v_t \tag{1}$$

s_t is the BCG artifact modeled as N^{th} order harmonic series

$$s_t = \mu_o + \mu_1 t + \sum_{r=1}^{N} A_r \cos(\omega r t) + B_r \sin(\omega r t) \tag{2}$$

where N is the number of harmonics in the spectrum (Fig. 1A); $\omega\,(\mathrm{rad/sec})$, the fundamental frequency defining the harmonic template, is linked to the heart rate in Hz (Fig. 1C); A_r and B_r define amplitude and phase of r^{th} harmonic.

v_t is the oscillatory EEG signal modeled as a P^{th} order autoregressive process

$$v_t = \sum_{k=1}^{P} a_k v_{t-k} + \epsilon_t \tag{3}$$

where P is set to 3 to represent the spectral peak (2 poles) and the DC component of a given test oscillation (Fig. 1A), and the ϵ_t are independent Gaussian random variables with zero mean and variance σ_ϵ^2. The AR model allows us to capture true EEG oscillatory dynamics without biasing the algorithm towards activity in specific frequency bands. We assume the AR(p) model is stationary at all times.

The harmonic BCG and the autoregressive EEG models reflect the empirically observed overlap in spectral and amplitude features, but are distinct enough to decouple the BCG artifact from the true EEG test signal. With this model, the problem of estimating and removing the BCG artifact becomes one of identifying the parameters ω, $\boldsymbol{\beta} = [\mu_o, \mu_1, A_1, B_1 A_2, B_2, \ldots, A_N, B_N]^T$, $\boldsymbol{\alpha} = [a_1, a_2, \ldots, a_P]^T$, and σ_ϵ^2.

C. Algorithm

This estimation problem is essentially harmonic regression in the setting of correlated noise - as seen easily by rewriting the above model in regressor matrix notation:

$$\mathbf{y} = Z(\omega)\boldsymbol{\beta} + \mathbf{v} \tag{4}$$

where $\mathbf{y} = [y_{t_1}, y_{t_2}, \ldots, y_{t_T}]^T$, $\mathbf{s} = Z(\omega)\boldsymbol{\beta}$, $Z(\omega)$ is:

$$\begin{bmatrix} 1 & cos(\omega t_1) & sin(\omega t_1) & \cdots & cos(N\omega t_1) & sin(N\omega t_1) \\ 1 & cos(\omega t_2) & sin(\omega t_2) & \cdots & cos(N\omega t_2) & sin(N\omega t_2) \\ \vdots & \vdots & \vdots & \ddots & \vdots & \vdots \\ 1 & cos(\omega t_T) & sin(\omega t_T) & \cdots & cos(N\omega t_T) & sin(N\omega t_T) \end{bmatrix}$$

and $\mathbf{v} = [v_{t_1}, v_{t_2}, \ldots, v_{t_T}]^T$ is multivariate Gaussian (0 mean, AR covariance $Q_{T\times T}$) with Akaike Markovian form:

$$\begin{bmatrix} v_{t-1} \\ v_{t-2} \\ \vdots \\ v_{t-P} \end{bmatrix} = \begin{bmatrix} a_1 & a_2 & \cdots & a_p \\ 1 & 0 & \cdots & 0 \\ \vdots & \ddots & \ddots & \vdots \\ 0 & \cdots & 1 & 0 \end{bmatrix} \begin{bmatrix} v_{t-2} \\ v_{t-3} \\ \vdots \\ v_{t-P-1} \end{bmatrix} + \begin{bmatrix} \epsilon_{t-1} \\ \epsilon_{t-2} \\ \vdots \\ \epsilon_{t-P} \end{bmatrix} \tag{5}$$

Maximum likelihood techniques work well in such parametric estimation problems [10]–[12]. By the maximum likelihood criterion, the best parameter estimates are those that, for an observed $T \times 1$ data vector $\mathbf{y}$, minimize:

$$-2\log L(\omega, \boldsymbol{\beta}, \boldsymbol{\alpha}, \sigma_\epsilon^2|\mathbf{y}) = T\log(\sigma_\epsilon^2) + \log(|Q|) + \frac{S_T}{\sigma_\epsilon^2} \tag{6}$$

where $S_T = (\mathbf{y} - Z(\omega)\boldsymbol{\beta})^T Q^{-1}(\mathbf{y} - Z(\omega)\boldsymbol{\beta})$. Maximizing over σ_ϵ^2 gives the concentrated likelihood cost C to minimize:

$$C(\omega, \boldsymbol{\beta}, \boldsymbol{\alpha}|\mathbf{y}) = T\log\left(\frac{S_T}{T}\right) + \log(\det(Q)) \tag{7}$$

D. Implementation & Data Analysis

This minimization can be implemented with a Newton's procedure that breaks down the complex nonlinear optimization into a series of sub-problems [10]–[12] which, when solved, converge to the global optimum [10], [13]. For a given $\boldsymbol{\alpha} = \tilde{\boldsymbol{\alpha}}$ and $\omega = \tilde{\omega}$, the best estimate $\hat{\boldsymbol{\beta}} = \arg\min C(\boldsymbol{\beta}, \tilde{\boldsymbol{\alpha}}, \tilde{\omega}|\mathbf{y})$, is given by generalized least squares on Eq. 4:

$$\begin{aligned} \hat{\boldsymbol{\beta}}(\tilde{\boldsymbol{\alpha}}, \tilde{\omega}) &= [Z^T(\tilde{\omega})Q^{(-1)}Z(\tilde{\omega})]^{(-1)}Z^T(\tilde{\omega})Q^{(-1)}\mathbf{y} \quad (8) \\ &= [Z^*(\tilde{\omega})^T Z^*(\tilde{\omega})]^{(-1)}Z^*(\tilde{\omega})^T\mathbf{y}^* \quad (9) \\ \hat{S_T}(\hat{\boldsymbol{\beta}}, \tilde{\omega}) &= (\mathbf{y}^* - Z^*(\tilde{\omega})\hat{\boldsymbol{\beta}})^T(\mathbf{y}^* - Z^*(\tilde{\omega})\hat{\boldsymbol{\beta}}) \quad (10) \end{aligned}$$

where Eqs. 9-10 are obtained by factorizing $Q^{(-1)}$ as $L^T L$ and denoting $Z^* = LZ, \mathbf{y}^* = L\mathbf{y}$. Substituting $\hat{S_T}(\hat{\boldsymbol{\beta}}, \tilde{\omega})$ into Eq. 7 concentrates the likelihood over $\boldsymbol{\beta}$

$$\bar{C}(\tilde{\boldsymbol{\alpha}}, \tilde{\omega}|\mathbf{y}) = T\log\left(\frac{\hat{S_T}(\hat{\boldsymbol{\beta}}, \tilde{\omega})}{T}\right) + \log(\det(Q)) \tag{11}$$

For a given $\tilde{\boldsymbol{\alpha}}$ and $\tilde{\omega}$, computing the cost (Eqs. 8-11) requires computing $y^*, Z^*, \det(Q) = |Q|$. This can be done efficiently with Kalman filters [10]–[12] - which we adapt for our AR(P) + harmonics model. Denote $M = [Z(\tilde{\omega})\ \mathbf{y}]$ and $M^* = [Z^*(\tilde{\omega})\ \mathbf{y}^*]$. For $j = 1, \ldots 2N+2$, $\mathbf{m}^* = j^{\text{th}}$ column of M^* can be computed by defining an observation vector $\mathbf{m} = j^{\text{th}}$ column of M, a $P \times 1$ state vector $\boldsymbol{\theta}_t$ and the state space model:

$$\boldsymbol{\theta}_t = A(\tilde{\boldsymbol{\alpha}})\boldsymbol{\theta}_{t-1} + N(0, I_{P\times P}) \text{ and } \mathrm{m_t} = \mathrm{B}\theta_\mathrm{t} \tag{12}$$

where A is the $P \times P$ matrix in Eq. 5 and $B = [1, 0, \ldots, 0]$. Denoting the predicted state estimate and estimate covariance from the Kalman filter as $\boldsymbol{\theta}_{t|t-1}$ and $P_{t|t-1}$, we get:

$$|Q| = \prod_{t=1}^{T} BP_{t|t-1} \text{ and } \mathrm{m_t^*} = \frac{(\mathrm{m_t} - \mathrm{B}\boldsymbol{\theta}_{\mathrm{t|t-1}})}{\sqrt{\mathrm{BP_{t|t-1}}}} \tag{13}$$

as detailed in [10], [11]. Thus, using the Kalman filter helps avoid explicit matrix multiplications, inverses, and orthogonalizations. Running this filter across all j gives $\mathbf{y}^*, Z^*, |Q|$. Substituting these into Eqs. 8-11 gives the cost $\bar{C}$ to minimize.

The numerical optimization of $\bar{C}$ over $\boldsymbol{\alpha}$ and ω is implemented with a genetic algorithm (Mathworks, Natick, MA). The ω search space is physiologically bounded based on the subject's clinical heart rate range. Bounds for α values are set to $0.2 - 5$ times the AR coefficients obtained by fitting the full data vector $\mathbf{y}$ to an AR(P) model. The elite count is limited to 3 of 150 individuals in a population, mutation and crossover factors were set to 80% and 20% respectively.

The numerically obtained optimal parameter estimates $\hat{\boldsymbol{\alpha}}$ and $\hat{\omega}$ are used to re-evaluate Eqs.8-13 to get the associated optimal $\hat{\boldsymbol{\beta}}$ and $\hat{S_T}$. Lastly, Eq.7 gives the optimal $\hat{\sigma_\epsilon^2} = \frac{\hat{S_T}}{T}$.

We apply the above maximum likelihood approach segment by segment on BCG-corrupted EEG data $\mathbf{y}$ and obtain model parameter estimates $\hat{\omega}$, $\hat{\boldsymbol{\beta}}$, $\hat{\boldsymbol{\alpha}}$, $\hat{\sigma_\epsilon^2}$. With these estimated parameters, we compute estimates for the BCG artifact ($\hat{s}_t$), EEG oscillation ($\hat{v}_t$), and residual noise ($\hat{\epsilon}_t$) time series.

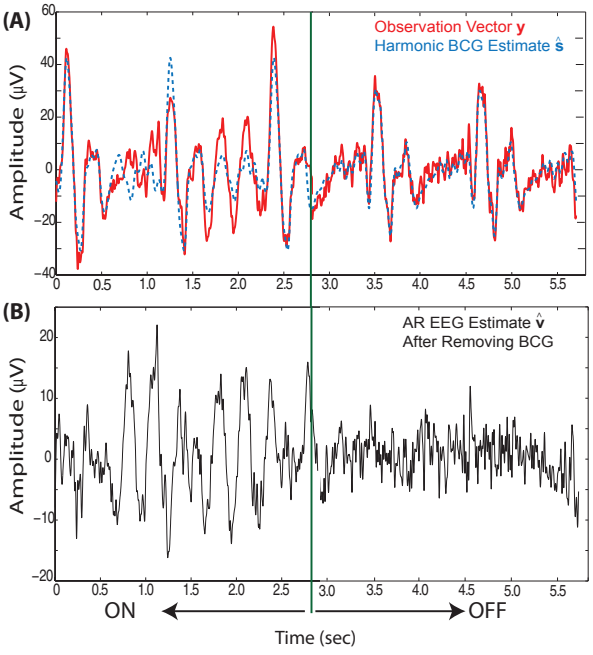

Fig. 2: Time Domain Estimates - (A) Red plot is the BCG-corrupted EEG oscillation $\mathbf{y}$ under test, and dashed blue plot is the estimated harmonic artifact $\hat{\mathbf{s}}$. (B) Time Series of the estimated oscillatory EEG component $\hat{\mathbf{v}}$. (A vs. B) Removing BCG makes the δ band ON/OFF pattern clearer.

III. Results

Fig. 2 shows time domain estimates for the BCG-corrupted EEG oscillation test case illustrated in Fig. 1. Panel 2A overlays a segment of the BCG-corrupted EEG oscillation ($\mathbf{y}$) and the corresponding estimated BCG artifact ($\hat{\mathbf{s}}$). It is evident that the BCG artifact comprises a large proportion of the power in the corrupted EEG oscillation - consistent with our driving hypothesis that the data roughly follows a harmonic template. Panel 2B shows the estimated oscillatory EEG component ($\hat{\mathbf{v}}$) – this estimate appears to have period of $3-4$ Hz showing that the AR model effectively preserves the temporal structure of the δ band EEG oscillation under test. Further, a Ljung-Box goodness of fit test on residuals ϵ, confirms whiteness ($p < 0.05$) – indicating that our model and approach explain the data effectively. The spectrogram of the estimated EEG oscillation component $\hat{\mathbf{v}}$) is shown in Fig. 3. Comparing this cleaned spectrogram (Fig. 3) with that of the corresponding BCG-corrupted EEG oscillation (Fig. 1B), we note that the algorithm effectively removes BCG artifacts. Our algorithm enables a 20-fold SNR improvement over the BCG-corrupted EEG oscillation (Fig. 1B vs. Fig. 3). Further the cleaned spectrogram has the same δ band spectral signatures as the test oscillation (in Fig. 1A). Specifically, the onset of δ band power changes matches the simulated test-case. Overall, this validates that the algorithm effectively restores ground-truth oscillatory signatures in EEG acquired at 3T. The SNR improvement is consistently over 10-fold across test cases.

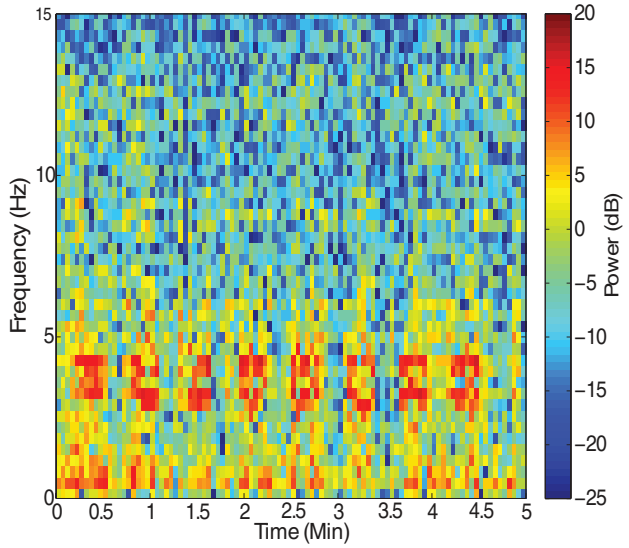

Fig. 3: Harmonic Regression Algorithm Removes BCG Artifact to Effectively Restore True EEG Oscillatory Signatures: Spectrogram after removing BCG artifacts from data of Fig.1B. The $3-4$ Hz band ON/OFF pattern of the corresponding uncorrupted test-case (Fig. 1A) is recovered. Onset and offset times of δ band power changes match with Fig. 1A.

IV. Discussion and Conclusion

We derived a novel reference-free algorithm that is highly effective in removing BCG artifacts from EEG oscillations recorded in MRI scanner. We have shown that the algorithm's estimates of underlying EEG oscillations reflect both overall pattern trends as well as specific timing and power changes in test oscillatory EEG signals. EEG oscillatory signatures estimated by our algorithm consistently have over $10-20$ fold increase in SNR over their BCG-corrupted counterparts, even in the lowest raw data SNR cases. This is unlike reference-based methods which sometimes even reduce SNR due to large residuals [1], [2]. Further, unlike subtraction or basis decomposition techniques that require long segments of continuous contaminated recordings to estimate the BCG artifact [1], [6], our technique works well even on short data segments. As our approach is based on a parametric model, we suggest that it may be well-poised to cope with time or stimulus dependent variations in BCG features including heart rate. One drawback of our method is that it is computationally intensive due to repeat runs of the Kalman filter during the numerical optimization. Future reports will explore ways to improve computational efficiency, apply the technique to clinical datasets, and study adaptations to different experimental and data acquisition paradigms.

References

[1] P. J. Allen, G. Polizzi, K. Krakow, D. R. Fish, and L. Lemieux, "Identification of EEG events in the MR scanner: the problem of pulse artifact and a method for its subtraction.," *NeuroImage*, vol. 8, pp. 229–39, Oct. 1998.

[2] G. Bonmassar, "Motion and Ballistocardiogram Artifact Removal for Interleaved Recording of EEG and EPs during MRI," *NeuroImage*, vol. 16, pp. 1127–1141, Aug. 2002.

[3] R. K. Niazy, C. F. Beckmann, G. D. Iannetti, J. M. Brady, and S. M. Smith, "Removal of FMRI environment artifacts from EEG data using optimal basis sets.," *NeuroImage*, vol. 28, pp. 720–37, Nov. 2005.

[4] M. L. Ellingson, E. Liebenthal, M. V. Spanaki, T. E. Prieto, J. R. Binder, and K. M. Ropella, "Ballistocardiogram artifact reduction in the simultaneous acquisition of auditory ERPS and fMRI.," *NeuroImage*, vol. 22, pp. 1534–42, Aug. 2004.

[5] K. H. Kim, H. W. Yoon, and H. W. Park, "Improved ballistocardiac artifact removal from the electroencephalogram recorded in fMRI.," *Journal of neuroscience methods*, vol. 135, pp. 193–203, May 2004.

[6] G. Srivastava, S. Crottaz-Herbette, K. M. Lau, G. H. Glover, and V. Menon, "ICA-based procedures for removing ballistocardiogram artifacts from EEG data acquired in the MRI scanner.," *NeuroImage*, vol. 24, pp. 50–60, Jan. 2005.

[7] W. Nakamura, K. Anami, T. Mori, O. Saitoh, A. Cichocki, and S.-i. Amari, "Removal of ballistocardiogram artifacts from simultaneously recorded EEG and fMRI data using independent component analysis.," *IEEE Trans. Biomed. Engg.*, vol. 53, pp. 1294–308, July 2006.

[8] K. Vanderperren, J. Ramautar, N. Novitski, and M. D. Vos, "Bcg artifacts in simultaneous eeg- fmri acquisitions," *International Journal of Bioelectromagnetism*, vol. 9, no. 3, pp. 146–150, 2007.

[9] P. L. Purdon, H. Millan, P. L. Fuller, and G. Bonmassar, "An Open-Source Hardware and Software System for Acquisition and Real-Time Processing of Electrophysiology during High Field MRI," *J. Neurosci Methods*, vol. 175, no. 2, pp. 165–186, 2008.

[10] C. F. Ansley and E. Wecker, "The Signal Extraction Regression Approach and Spline to Nonlinear Smoothing," *Journal of American Statistical Association*, vol. 78, no. 381, pp. 81–89, 1983.

[11] E. N. Brown and C. H. Schmid, "Application of the Kalman Filter to Computational Problems in Statistics," in *Methods in Enzymology*, vol. 240, pp. 171–181, 1994.

[12] E. N. Brown, V. Solo, Y. Choe, and Z. Zhang, "Measuring period of human biological clock: infill asymptotic analysis of harmonic regression parameter estimates.," *Methods in enzymology*, vol. 383, pp. 382–405, Jan. 2004.

[13] C. Corradi, "A Note on the Computation of MAximum Likelihood Estimates in Linear Regression Models with Autocorrelated Errors," *Journal of Econometrics*, vol. 11, pp. 303–317, 1979.